




Calcium dynamics in tomato pollen tubes using the Yellow Cameleon 3.6 sensor

María Laura Barberini¹ · Lorena Sigaut² · Weijie Huang^{3,7} · Silvina Mangano⁴ · Silvina Paola Denita Juarez⁴ · Eliana Marzol⁴ · José Estevez⁴ · Mariana Obertello¹ · Lía Pietrasanta^{2,5} · Weihua Tang³ · Jorge Muschietti^{1,6} 

Received: 17 November 2016 / Accepted: 4 December 2017
© Springer-Verlag GmbH Germany, part of Springer Nature 2017

Key message *In vitro* tomato pollen tubes show a cytoplasmic calcium gradient that oscillates with the same period as growth.

Abstract Pollen tube growth requires coordination between the tip-focused cytoplasmic calcium concentration ($[Ca^{2+}]_{cyt}$) gradient and the actin cytoskeleton. This $[Ca^{2+}]_{cyt}$ gradient is necessary for exocytosis of small vesicles, which contributes to the delivery of new membrane and cell wall at the pollen tube tip. The mechanisms that generate and maintain this $[Ca^{2+}]_{cyt}$ gradient are not completely understood. Here, we studied calcium dynamics in tomato (*Solanum lycopersicum*) pollen tubes using transgenic tomato plants expressing the *Yellow Cameleon 3.6* gene under the pollen-specific promoter *LAT52*. We use tomato as an experimental model because tomato is a Solanaceous plant that is easy to transform, and has an excellent genomic database and genetic stock center, and unlike Arabidopsis, tomato pollen is a good system to do biochemistry. We found that tomato pollen tubes showed an oscillating tip-focused $[Ca^{2+}]_{cyt}$ gradient with the same period as growth. Then, we used a pharmacological approach to disturb the intracellular Ca^{2+} homeostasis, evaluating how the $[Ca^{2+}]_{cyt}$ gradient, pollen germination and *in vitro* pollen tube growth were affected. We found that cyclopiazonic acid (CPA), a drug that inhibits plant P_{IIA} -type Ca^{2+} -ATPases, increased $[Ca^{2+}]_{cyt}$ in the subapical zone, leading to the disappearance of the Ca^{2+} oscillations and inhibition of pollen tube growth. In contrast, 2-aminoethoxydiphenyl borate (2-APB), an inhibitor of Ca^{2+} released from the endoplasmic reticulum to the cytoplasm in animals cells, completely reduced $[Ca^{2+}]_{cyt}$ at the tip of the tube, blocked the gradient and arrested pollen tube growth. Although both drugs have antagonistic effects on $[Ca^{2+}]_{cyt}$, both inhibited pollen tube growth triggering the disappearance of the $[Ca^{2+}]_{cyt}$ gradient. When CPA and 2-APB were combined, their individual inhibitory effects on pollen tube growth were partially compensated. Finally, we found that GsMTx-4, a peptide from spider venom that blocks stretch-activated Ca^{2+} channels, inhibited tomato pollen germination and had a heterogeneous effect on pollen tube growth, suggesting that these channels are also involved in the maintenance of the $[Ca^{2+}]_{cyt}$ gradient. All these results indicate that tomato pollen tube is an excellent model to study calcium dynamics.

Keywords Calcium concentration gradient · Pollen tube growth · *Solanum lycopersicum* · Yellow Cameleon 3.6 · Ion channels · Calcium ATPases

Abbreviations

2-APB 2-Aminoethoxydiphenyl borate
 $[Ca^{2+}]_{cyt}$ Cytoplasmic calcium concentration
CPA Cyclopiazonic acid

cpVenus Circularly permuted Venus
DIC Differential interference contrast
DMSO Dimethyl sulfoxide
ECFP Enhanced cyan fluorescent protein
ER Endoplasmic reticulum
FRET Fluorescence resonance energy transfer
IP₃ Inositol triphosphate
PEG Polyethylene glycol
PGM Pollen germination medium
YC Yellow Cameleon

Communicated by Zhenbiao Yang.

Electronic supplementary material The online version of this article (<https://doi.org/10.1007/s00497-017-0317-y>) contains supplementary material, which is available to authorized users.

✉ Jorge Muschietti
prometeo@dna.uba.ar

Extended author information available on the last page of the article

Introduction

Pollen tubes are essential components of sexual reproduction in higher plants. They transport and deliver the two sperm cells to the ovules, where fertilization takes place. In many species, in vitro pollen tube growth is oscillatory and delimited to the tip, requiring the coordination of several cellular processes such as ion fluxes, actin dynamics, vesicle trafficking and cell wall synthesis. Thus, the pollen tube is an excellent system to study polarized tip growth, cell–cell communication, ion channel activity and membrane and cytoskeleton dynamics. In *Lilium longiflorum*, a tip-focused $[Ca^{2+}]_{\text{cyt}}$ gradient is established and maintained during in vitro pollen tube growth, oscillating at the same period as growth, but at a different phase (Pierson et al. 1996; Holdaway-Clarke et al. 1997; Messerli and Robinson 1997). This gradient reaches a Ca^{2+} concentration of 10 μM at the tip, dropping to 200 nM as close as 20 μm from the tip (Messerli et al. 2000). A new computational approach allows to estimate tip location, track growth and analyze calcium oscillations at pollen tube tip with subpixel resolution (Damineli et al. 2017). The use of Ca^{2+} channel blockers or increasing Ca^{2+} in the growth media interferes with the $[Ca^{2+}]_{\text{cyt}}$ gradient and blocks pollen tube growth. In the case of uneven Ca^{2+} concentration at the tip, pollen tubes modify their growth direction toward the side where the concentration is higher (Malhó and Trewavas 1996).

The $[Ca^{2+}]_{\text{cyt}}$ gradient is controlled and maintained, in part, by specific Ca^{2+} channels localized in the plasma membrane of the pollen tube tip. Ligand (cyclic nucleotide and amino acid)-gated channels (Frietsch et al. 2007; Song et al. 2009; Michard et al. 2011; Wu et al. 2011; Gao et al. 2016), stretch-activated Ca^{2+} channels (Dutta and Robinson 2004; Hamilton et al. 2015) and voltage-dependent channels (Wang et al. 2004; Shang et al. 2005; Qu et al. 2007) are involved controlling the entry of extracellular Ca^{2+} into pollen tubes. In order to initiate a new growth cycle, pollen tubes should remove that high amount of Ca^{2+} away from the tip area. Ca^{2+} -ATPase pumps, such as Arabidopsis ACA9, would exclude Ca^{2+} from the pollen tube into the apoplast (Schiott et al. 2004). It is also reasonable to consider that storage of Ca^{2+} in intracellular compartments such as endoplasmic reticulum (ER), vacuoles or even mitochondria contributes to lower $[Ca^{2+}]_{\text{cyt}}$ (Holdaway-Clarke et al. 1997; Sze et al. 2000). This hypothesis is supported by the fact that cyclopiazonic acid (CPA), an inhibitor of the P_{IIA} -type Ca^{2+} -ATPases (ECAs), increased $[Ca^{2+}]_{\text{cyt}}$, decreased the $[Ca^{2+}]$ in the ER and subsequently blocked Arabidopsis pollen tube growth (Iwano et al. 2009). It has not been yet established whether pollen Ca^{2+} -ATPase pumps localized in any intracellular compartment would contribute to establishing a new round of $[Ca^{2+}]_{\text{cyt}}$ gradient.

In this paper, to study Ca^{2+} dynamics in pollen tubes, we used transgenic tomato plants expressing the *Yellow Cameleon 3.6* gene under the pollen-specific promoter *LAT52*. We also used drugs that disturb the intracellular Ca^{2+} homeostasis in plant cells, to study how the $[Ca^{2+}]_{\text{cyt}}$ gradient, pollen germination and in vitro pollen tube growth were affected.

Materials and methods

Plant material

Wild-type and *Yellow Cameleon 3.6*-expressing tomato plants were grown in soil in the greenhouse (25 °C, 16 h light). Mature pollen grains were collected by vibrating anthers of mature flowers with a biovortex (*BioSpec Products*).

Generation of transgenic *Yellow Cameleon 3.6* tomato

Tomato plants were transformed with a gene encoding the fluorescence resonance energy transfer (FRET)-based Ca^{2+} sensor *Yellow Cameleon 3.6* (YC 3.6) (Nagai et al. 2004), under the control of the pollen-specific promoter *LAT52* (Twell et al. 1990). *Agrobacterium tumefaciens* LBA4404 (Hoekema et al. 1984) harboring the binary vector pCAMBIA2300 with a pLAT52:YC3.6:35S-ter fragment was used to transform tomato as described (McCormick 1992).

Chemicals

Cyclopiazonic acid (CPA) and 2-aminoethoxydiphenyl borate (2-APB) were obtained from Calbiochem (La Jolla, CA, USA). A stock solution containing 12.5 mM of CPA was prepared dimethyl sulfoxide (DMSO). 2-APB was stored as a 100 mM stock solution in DMSO. GsMTx-4 was obtained from Alomone Labs (Jerusalem, Israel), and a 0.1 mM stock solution was prepared in distilled water. Working solutions were prepared by dilution with pollen germination medium (PGM). For each chemical treatment, a corresponding volume of solvent was used as control treatment.

In vitro pollen germination and pollen tube growth assays

In vitro germination assays were performed as described (Muschiatti et al. 1998). Briefly, pollen grains (1 mg mL^{-1}) were resuspended in pollen germination medium (PGM) [24% (w/v) polyethylene glycol (PEG) molecular weight 3350, 20 mM MES pH 6.0, 0.8 mM MgSO_4 , 1 mM KCl, 1.6 mM boric acid, 2.8 mM $\text{Ca}(\text{NO}_3)_2$ and 2.5% (w/v) sucrose]. For pollen germination assays, the inhibitors were

added together with PGM, and then, the pollen suspension was incubated for 1 h at 28 °C. For pollen tube growth assays, pollen was germinated for 1 h in PGM at 28 °C, followed by drug treatments for 1 h. The control for each drug treatment was done with germination medium supplemented with the solvent used.

Pollen grains and pollen tubes were observed using a BX41 microscope (*Olympus*) equipped with a 10× objective. All experiments were repeated three times ($n = 3$), and three technical replicates were carried out for each treatment. For each replicate, more than 500 pollen grains (obtained from five different plants) and 75 pollen tubes were analyzed to calculate pollen germination and pollen tube growth percentage, respectively. Pollen was considered germinated only when tube length was greater than the diameter of the pollen grain. To facilitate the analysis of pollen tube growth inhibition, we converted pollen tube length values to pollen tube growth percentage, considering the control mean length (untreated pollen tubes) as 100% pollen tube growth. Data were analyzed by analysis of the variance (ANOVA), and differences between means were compared with a Tukey's post hoc test.

Imaging of cytoplasmic Ca^{2+} levels

Pollen grains from YC 3.6-expressing plants were resuspended in PGM and placed in *Labtek* chambers. Pollen grains were germinated for 1 h at 28 °C, and then, inhibitors were added. Time-lapse imaging of pollen tubes was performed using an Olympus IX81 inverted microscope equipped with Olympus FV-1000 confocal unit. An Olympus UPlanSApo 60×, 1.2 numerical aperture, water immersion objective lens was used for imaging. The YC 3.6 was excited with the 440-nm line of the diode laser. The enhanced cyan fluorescent protein (ECFP) and FRET-dependent circularly permuted Venus (cpVenus) emission were collected using a 458-nm dichroic mirror, and 480–495- and 535–565-nm emission filters for ECFP and cpVenus, respectively. Differential interference contrast (DIC) images were acquired simultaneously. Images were collected every 5 s. For bleed-through determination, 35S promoter-ECFP-CaM or 35S promoter-M13-cpVenus constructs were generated in *E. coli* cells. For autofluorescence determination, wild-type pollen tubes were used.

Image and data analysis

Image analysis was performed as previously described (Barberini and Muschiatti 2015). All slices of the same pollen tube were aligned by its pollen tube tip using the Template Matching and Slice Alignment plug-in for ImageJ. This alignment takes in consideration the displacements in X and Y axes for each slice allowing the quantification of

pollen tube growth with a subpixel resolution (Barberini and Muschiatti 2015). The cpVenus/ECFP ratio was determined using the Ratio-plus plug-in for ImageJ, and fluorescence intensity was measured in $5\text{-}\mu\text{m}^2$ ROI at the pollen tube apex. Kymographs were generated by tracing a line along the pollen tube growth axis at one time point using the multi-kymograph plug-in for ImageJ. In the kymograph, each horizontal line of the kymograph represents the ratio (cpVenus/ECFP), while pollen tube length is represented on the horizontal axis and time on the vertical axis being the slope of the kymograph the growth rate of the pollen tube.

Results

Expression of YC 3.6 in tomato pollen

In order to study Ca^{2+} dynamics in growing pollen tubes, we used transgenic VF36 tomato plants expressing the FRET-based Ca^{2+} indicator *Yellow Cameleon 3.6* gene (Nagai et al. 2004), driven by the *LAT52* pollen-specific promoter (Twell et al. 1990). We first examined Ca^{2+} oscillations during in vitro pollen tube growth. To this end, pollen grains were cultured in a liquid germination medium (Muschiatti et al. 1998) and ECFP and FRET-dependent cpVenus fluorescence emission of pollen tubes were acquired at 5-s intervals, calculating the ratio cpVenus/ECFP in the apical and subapical pollen tube regions. Differential interference contrast (DIC) images were acquired simultaneously.

As previously described for tobacco (Michard et al. 2008) and lily (Holdaway-Clarke et al. 1997, 2003; Messerli et al. 2000; Cardenas et al. 2008), in vitro growing tomato pollen tubes showed an oscillating tip-focused $[\text{Ca}^{2+}]_{\text{cyt}}$ gradient (Figs. 1 and 2a). Both cpVenus/ECFP ratio and growth rate curves show similar period (Fig. 1). Ca^{2+} levels were highest within 10 μm distance from the tip and then decreased into the tube shank. Figure 2b shows dynamic changes in

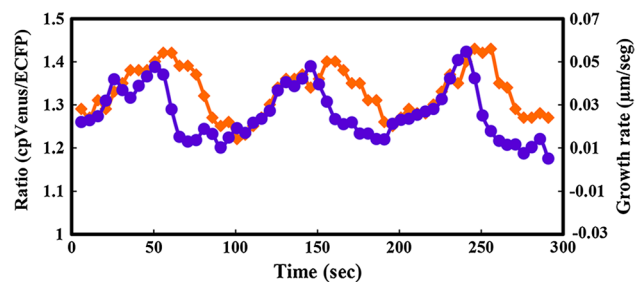


Fig. 1 Quantitative analysis of pollen tube growth and $[\text{Ca}^{2+}]_{\text{cyt}}$ at the tip area of tomato pollen tubes. The period and shape of cpVenus/ECFP ratio and growth rate curves are similar. The Ca^{2+} peak follows the growth rate peak. The cpVenus/ECFP ratio in pollen tip was measured in $5\text{-}\mu\text{m}^2$ ROI (orange line). The purple line corresponds to pollen tube growth rate

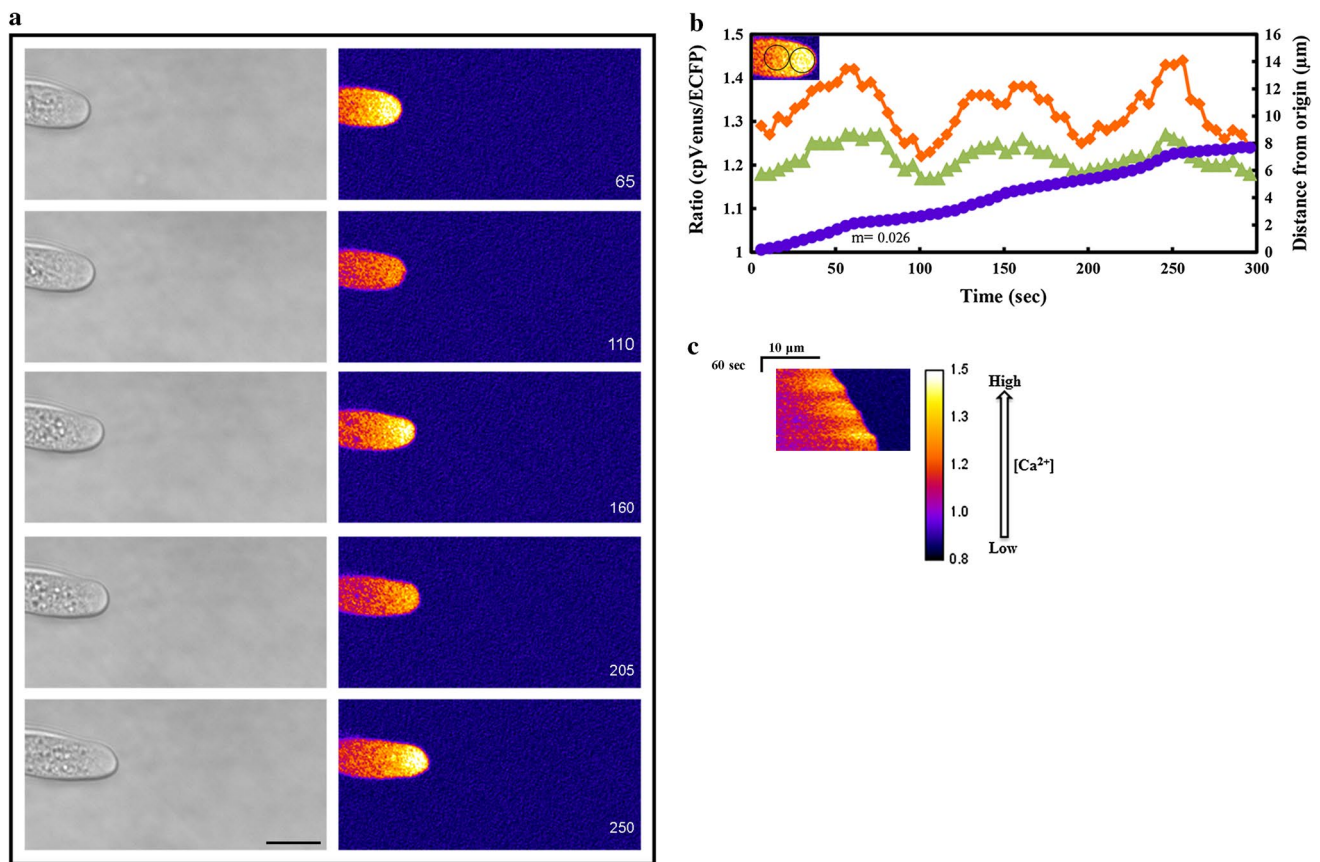


Fig. 2 Pollen growth and Ca^{2+} dynamics in tomato plants expressing YC 3.6 under the control of the pollen-specific promoter *LAT52*. **a** Time-lapse sequence shows the in vitro growth of a representative pollen tube (left panels) ($n = 10$). Fluorescence ratio imaging reveals a tip-focused $[\text{Ca}^{2+}]_{\text{cyt}}$ gradient. The fluorescence intensities were showed in pseudo-color coding (right panels). Numbers represent time in seconds. Scale bar represents $10 \mu\text{m}$. **b** Quantitative analysis of pollen tube growth and $[\text{Ca}^{2+}]_{\text{cyt}}$ in tomato pollen tubes growing in vitro condition. The ratios (cpVenus/ECFP) in apical (orange line) and subapical (green line) regions were measured in $5\text{-}\mu\text{m}^2$ ROIs (see

inset). The purple line corresponds to pollen tube elongation (“distance”). “ m ” is the slope that represents pollen growth rate during the experiment. **c** Kymograph of the tube presented in **a**. Each horizontal line of the kymograph illustrates ratio (cpVenus/ECFP) values along a line traced in the middle of the tube at one time point. Pollen tube length is represented on the horizontal axis of the kymograph and time on the vertical axis. The slope on the right side of the kymograph reflects the growth rate of the tube. The vertical colored bar illustrates the ratio cpVenus/ECFP

$[\text{Ca}^{2+}]_{\text{cyt}}$ at the apical and subapical regions and associated oscillations in pollen tube growth (See also Suppl. movie 1). In tomato, Ca^{2+} oscillated with a period of 65–100 s, while in lily the period was 15–46 s (Holdaway-Clarke et al. 1997, 2003; Messerli et al. 2000; Cardenas et al. 2008), in Arabidopsis 12–48 s (Iwano et al. 2004, 2009; Damineli et al. 2017) and in tobacco 1–4 min (Michard et al. 2008). The spatiotemporal dynamics of $[\text{Ca}^{2+}]_{\text{cyt}}$ gradient and tube growth is shown in the form of a kymograph (Fig. 2c).

Effects of CPA, 2-APB and GsMTx-4 on Ca^{2+} dynamics in tomato pollen tubes

Cyclopiazonic acid (CPA) is a specific inhibitor of animal SERCA type Ca^{2+} -ATPases (Seidler et al. 1989; Plenge-Tellechea et al. 1997; Martinez-Azorin 2004) and plant

P_{IIA} -type Ca^{2+} -ATPases (Liang and Sze 1998; Geisler et al. 2000; Sze et al. 2000). We analyzed the effects of CPA on tomato pollen germination and pollen tube growth. CPA inhibited pollen germination and arrested pollen tube growth in a dose-dependent manner (Fig. 3a). Specifically, $70 \mu\text{M}$ CPA reduced pollen tube growth to 52%. We found that CPA had a heterogeneous effect on pollen tube growth. Specifically, 60% of the tubes were irreversibly arrested, while the other 40% showed an initial period of inhibition with a later recovery of normal growth. Having demonstrated that CPA inhibited tomato pollen tube growth, we then monitored how CPA affects Ca^{2+} oscillations during pollen tube growth. Pollen tubes that were irreversibly arrested showed an increased $[\text{Ca}^{2+}]_{\text{cyt}}$ in the subapical zone when compared to control tubes, with the disappearance of the $[\text{Ca}^{2+}]_{\text{cyt}}$ gradient

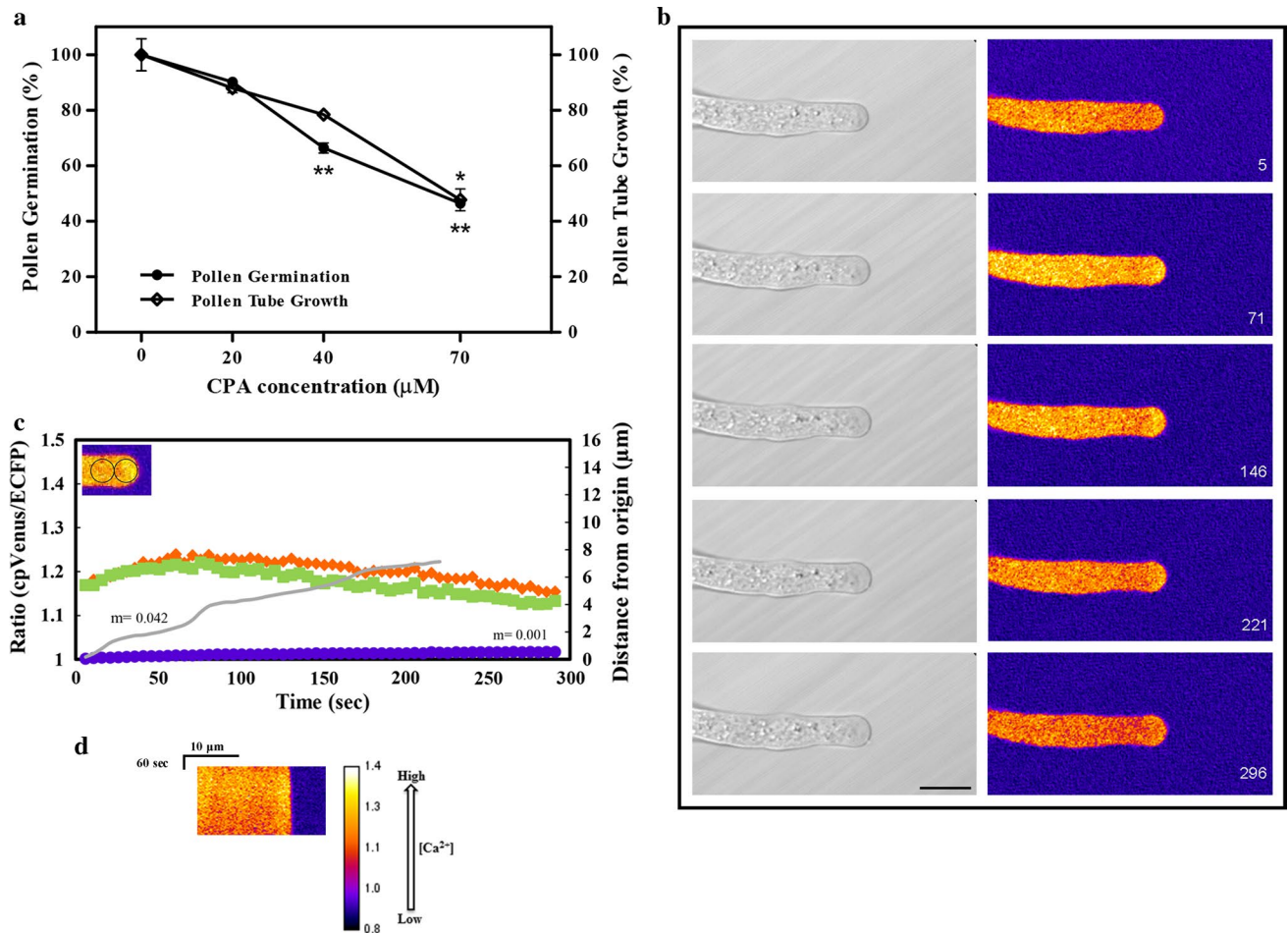


Fig. 3 Effects of CPA on tomato pollen germination, pollen tube growth and $[\text{Ca}^{2+}]_{\text{cyt}}$ oscillations in YC 3.6 tomato plants. **a** CPA reduces pollen germination and inhibits pollen tube growth. Data were presented as mean \pm SEM from three independent experiments. Asterisks indicate significant differences between control (untreated pollen) and CPA treatment by Tukey's post hoc test ($*p < 0.05$ and $**p < 0.01$). **b** Effects of 50 μM CPA on pollen growth and Ca^{2+} dynamics. Time-lapse sequence shows the growth inhibition of a representative pollen tube (left panels) ($n = 10$). Fluorescence ratio imaging reveals an increase of the $[\text{Ca}^{2+}]_{\text{cyt}}$ in the subapical zone. The fluorescence intensities are in pseudo-color coding (right pan-

els). Numbers represent time in seconds, where zero seconds corresponds to 20 min after CPA is added. Scale bar represents 10 μm . **c** Quantitative analysis of pollen tube growth and $[\text{Ca}^{2+}]_{\text{cyt}}$ in tomato pollen tubes after the addition of CPA. The ratios (cpVenus/ECFP) in apical (orange line) and subapical (green line) regions were measured in 5- μm^2 ROIs (see inset). The purple line corresponds to pollen tube elongation in the presence of CPA. Solid gray line represents pollen tube elongation of control pollen (treated with solvent). "m" is the slope that represents pollen growth rate during the experiment. **d** Kymograph of the pollen tube presented in **b**. The vertical colored bar illustrates the ratio cpVenus/ECFP

and growth inhibition (compare the slope $m = 0.001$ to $m = 0.042$ for the control tube in Fig. 3c) (Fig. 3b, c and Suppl. Movie 2). The kymograph (Fig. 3d) showed a slight slope due to the lower growth rate together with homogeneous $[\text{Ca}^{2+}]_{\text{cyt}}$ from the tip into the subapical zone (compared with the kymograph from Fig. 2c). Considering that CPA inhibits plant P_{IIA} -type Ca^{2+} -ATPases, these results suggest that tomato pollen tubes contain CPA-sensitive Ca^{2+} -ATPases that would control Ca^{2+} storage during pollen tube growth. Figure 4 shows that the fluorescent signals of a CPA-treated tube at the tip and along the shank were comparable and higher to the signal observed at the subapical zone of a control tube.

We next analyzed the effect of 2-aminoethoxydiphenyl borate (2-APB), a drug that in animal cells negatively affects release of Ca^{2+} from the ER into the cytoplasm, thereby inhibiting the inositol triphosphate (IP_3) receptor (Maruyama et al. 1997). Figure 5a shows that 5 μM of 2-APB reduced statistically pollen germination to 65%, while the inhibition was almost complete using 10 μM . We also observed a dose-dependent inhibition of pollen tube growth when 2.5–3.75 μM of 2-APB was used (Fig. 5a). Treatment with 2.5 μM 2-APB for 5 min (Fig. 5b) reduced $[\text{Ca}^{2+}]_{\text{cyt}}$ at both apical and subapical regions of the tube when compared to a control tube (Fig. 4). This result, together with the loss of the $[\text{Ca}^{2+}]_{\text{cyt}}$ oscillatory gradient, generated

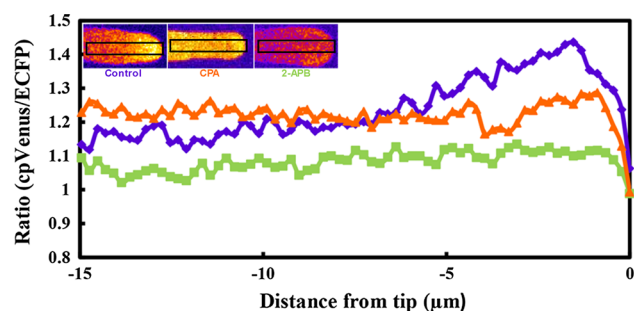


Fig. 4 Effects of CPA and 2-APB on the $[Ca^{2+}]_{cyt}$ fluorescent signals in tomato pollen tubes. The ratios (cpVenus/ECFP) in control (purple line), CPA (orange line)- and 2-APB (green line)-treated pollen tubes were measured in ROIs that scan down the tubes from the tip to the shank (see insets). One representative pollen tube is shown for each treatment

a permanent inhibition of pollen tube growth (compare the slope $m = 0.006$ to $m = 0.022$ for the control tube in Fig. 5c). The kymograph (Fig. 5d) shows the slight slope of the growth rate together with low and stable $[Ca^{2+}]_{cyt}$ from the tip into the subapical zone. Considering that in animal cells 2-APB inhibits the release of Ca^{2+} from the ER, our results suggest that pollen tubes should contain a similar mechanism controlling Ca^{2+} release into pollen tube cytoplasm. Results obtained with CPA and 2-APB suggest that an unregulated increase or decrease of $[Ca^{2+}]_{cyt}$ affects pollen tube growth because in both cases, the $[Ca^{2+}]_{cyt}$ gradient is disturbed.

Considering that CPA and 2-APB have antagonistic effects on $[Ca^{2+}]_{cyt}$, we analyzed whether the simultaneous addition of both drugs could compensate their individual inhibitory effects on pollen tube growth. Table 1 shows that 20 μM of CPA together with 2.5 μM of 2-APB partially reverted the inhibitory effect of 2.5 μM of 2-APB alone. The same effect was found when 30 μM of CPA was used together with 1.25 μM of 2-APB (Table 1). These results suggest that the inhibitory effect of 2-APB on pollen tube growth is partially compensated by CPA.

Pollen tubes have in their plasma membrane different calcium channels responsible for Ca^{2+} entry into the pollen tube (Dutta and Robinson 2004; Shang et al. 2005; Frietsch et al. 2007; Qu et al. 2007; Michard et al. 2011; Wu et al. 2011; Hepler et al. 2012; Gao et al. 2016). In *L. longiflorum* pollen tube tip protoplasts, the crude venom of the spider *Grammostola spatulata* that blocks stretch-activated channels in animals inhibited lily pollen tube growth by stopping the Ca^{2+} influx (Dutta and Robinson 2004). To test whether mechanosensitive channels are involved in the regulation of tomato pollen germination and tube growth, we used GsMTx-4, an active peptide

from the spider's venom that specifically blocks mechanosensitive channels in animal cells (Suchyna et al. 2000). Our results showed that GsMTx-4 inhibited pollen germination and arrested pollen tube growth (Fig. 6a). However, the effect of GsMTx-4 on pollen tube growth was heterogeneous. Some pollen tubes were inhibited, whereas others elongated as untreated tubes, suggesting that other type of channels could participate in the regulation of the calcium intake. Pollen tubes affected by GsMTx-4 showed a complete decrease of the $[Ca^{2+}]_{cyt}$ at the pollen tube tip and the disappearance of the oscillatory calcium concentration gradient (Fig. 6b), while pollen tube growth was inhibited (compare the slope $m = 0.001$ to $m = 0.033$ for the control tube in Fig. 6c). The kymograph (Fig. 6d) showed the abolition of the slope denoting the inhibition of the growth rate together with the decrease of the $[Ca^{2+}]_{cyt}$ from the tip into the subapical zone. These results suggest that stretch-activated Ca^{2+} channels are potentially involved in the entry of calcium to the pollen cytoplasm and therefore in the maintenance of the calcium concentration gradient.

Discussion

It has been described in several plant species that in vitro pollen tube growth is coupled with a $[Ca^{2+}]_{cyt}$ gradient necessary for a correct polarized secretion, arrangement of the actin cytoskeleton, movement of organelles and biochemical activity essential for pollen tube growth (Hepler and Winship 2015). Recently, computational approaches have been used to estimate tip location with subpixel resolution improving pollen tube growth and $[Ca^{2+}]_{cyt}$ oscillations measurements (Damineli et al. 2017). In this work, we described that tomato pollen tubes showed a tip-focused $[Ca^{2+}]_{cyt}$ gradient with Ca^{2+} oscillations associated with pollen tube growth. Even though regular oscillations have been described in lily, tobacco, petunia and tomato in vitro growing pollen tubes (Holdaway-Clarke et al. 1997, 2003; Geitmann and Cresti 1998; Messerli et al. 2000; Cardenas et al. 2008; Michard et al. 2008), only Arabidopsis pollen tubes growing in vitro with slow or stopped growth showed regular $[Ca^{2+}]_{cyt}$ oscillations (Iwano et al. 2009; Damineli et al. 2017). Moreover, normal in vivo growing Arabidopsis pollen tubes showed no $[Ca^{2+}]_{cyt}$ oscillations (Iwano et al. 2009) revealing the complexity of the regulation of calcium dynamics during pollen tube tip growth.

In order to study the mobilization of Ca^{2+} during pollen tube growth, we used specific drugs. First, we used cyclopiazonic acid (CPA), a drug that inhibits

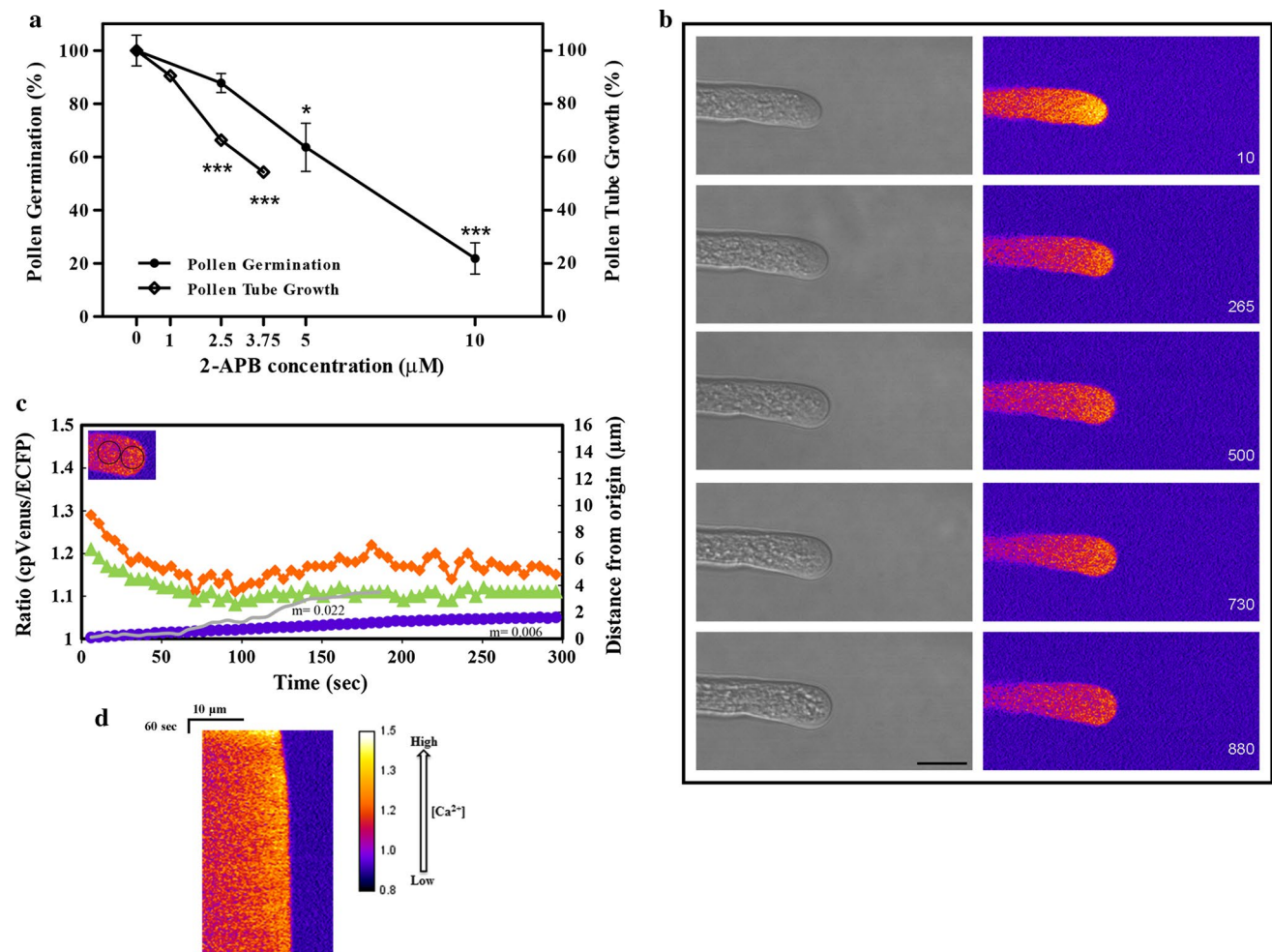


Fig. 5 Effects of 2-APB on tomato pollen germination, pollen tube growth and $[\text{Ca}^{2+}]_{\text{cyt}}$ oscillations in YC 3.6 tomato plants. **a** 2-APB reduces pollen germination and inhibits pollen tube growth. Data were presented as mean \pm SEM from three independent experiments. Asterisks indicate significant differences between control (non-treated) and 2-APB treatment by Tukey's post hoc test ($*p < 0.05$ and $***p < 0.001$). **b** Effects of 2.5 μM 2-APB on pollen growth and Ca^{2+} dynamics. Time-lapse sequence shows the growth inhibition of a representative pollen tube (left panels) ($n = 10$). Fluorescence ratio imaging reveals a decrease of the $[\text{Ca}^{2+}]_{\text{cyt}}$ in the apical zone and dissipation of the Ca^{2+} concentration gradient. The fluorescence intensities were presented in pseudo-color coding (right panels). Numbers

represent time in seconds, where zero seconds corresponds to 5 min after the drug is added. Scale bar represents 10 μm . **c** Quantitative analysis of pollen tube growth and $[\text{Ca}^{2+}]_{\text{cyt}}$ in tomato pollen tubes after the addition of 2-APB. The ratio (cpVenus/ECFP) in apical (orange line) and subapical (green line) region was measured in 5- μm^2 ROIs (see inset). The purple line corresponds to pollen tube elongation in the presence of 2-APB. Solid gray line represents the pollen tube elongation of control pollen (treated with solvent). "m" is the slope that represents of pollen growth rate during experiment. **d** Kymograph of the pollen tube presented in **b**. The vertical colored bar illustrates the ratio cpVenus/ECFP

animal SERCA type Ca^{2+} -ATPases (Seidler et al. 1989; Plenge-Tellechea et al. 1997; Martinez-Azorin 2004) and P_{IIA} -type plant Ca^{2+} -ATPases (ECAs) (Liang and Sze 1998; Geisler et al. 2000; Sze et al. 2000). Specifically, it has been reported that when expressed in yeast, ECA1, an ER Ca^{2+} -ATPase from Arabidopsis, was inhibited by CPA although the mechanism is still unclear (Liang and Sze 1998). Moreover, CPA increased $[\text{Ca}^{2+}]_{\text{cyt}}$ in Arabidopsis

roots (Zhang et al. 2011), lowered $[\text{Ca}^{2+}]$ in the ER in Arabidopsis root tip cells (Bonza et al. 2013) and inhibited Ca^{2+} spiking during nodulation in *Sesbania rostrata* (Capoen et al. 2009) and *Medicago truncatula* (Engstrom et al. 2002). We found that 50 μM CPA blocked tomato pollen germination and pollen tube growth, inducing high levels of Ca^{2+} in the subapical zone that marked the disappearance of the tip-focused $[\text{Ca}^{2+}]_{\text{cyt}}$ gradient and

Table 1 Effects of the combination of CPA and 2-APB on pollen tube growth

Treatment	Pollen tube growth (%)
CPA 20 μ M	92.7 \pm 1.46 ^(a)
2-APB 2.5 μ M	58.6 \pm 1.77 ^(b)
Combination	75.48 \pm 2.66 ^(c)
CPA 30 μ M	84.84 \pm 1.1 ^(a)
2-APB 1.25 μ M	66.63 \pm 1.97 ^(b)
Combination	73.88 \pm 1.71 ^(c)

Results are expressed as a pollen tube growth percentage considering the control mean length as 100% pollen tube growth. Data represent the mean values \pm SEM of three replicates. Different letters indicate significant difference among treatments (p values were: $p < 0.01$, one-way ANOVA, Tukey's test)

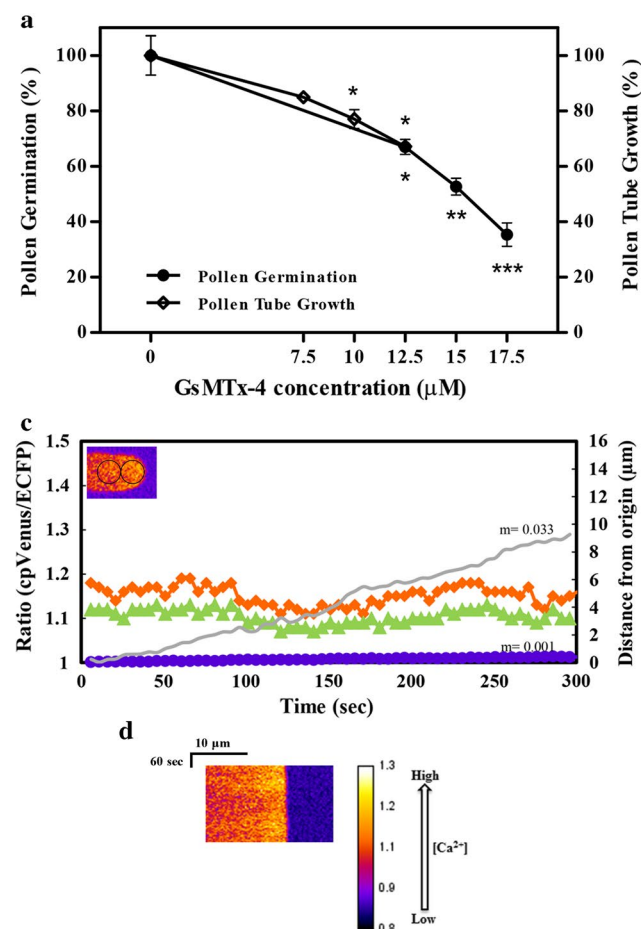
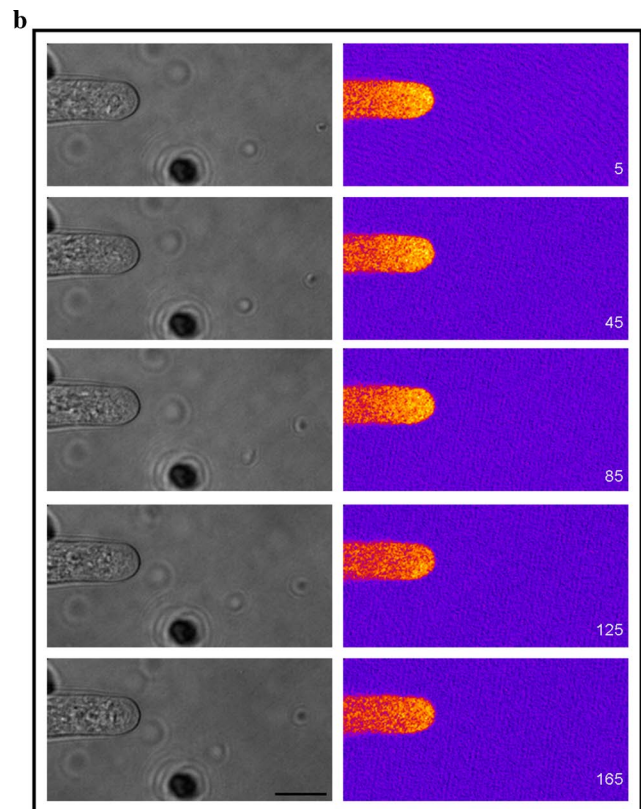


Fig. 6 Effects of GsMTx-4 on tomato pollen germination, pollen tube growth and [Ca²⁺]_{cyt} oscillations in YC 3.6 tomato plants. **a** GsMTx-4 reduces pollen germination and inhibits pollen tube growth. Data were presented as mean \pm SEM from three independent experiments. Asterisks indicate significant differences between control (non-treated) and GsMTx-4 treatment by Tukey's post hoc test (* $p < 0.05$, ** $p < 0.01$ and *** $p < 0.001$). **b** Effects of 12.5 μ M GsMTx-4 on pollen tube growth and Ca²⁺ dynamics. Time-lapse sequence shows the growth inhibition of a representative pollen tube (left panels) ($n = 10$). Fluorescence ratio imaging reveals a decrease of the [Ca²⁺]_{cyt} in the apical zone and disappearance of the calcium concentration gradient. The fluorescence intensities were presented

the subsequent inhibition of the Ca²⁺ oscillations. Our results are consistent with those observed in Arabidopsis pollen tubes where 10 μ M CPA inhibited semi-in vivo growth, increased the high [Ca²⁺]_{cyt} area while decreasing [Ca²⁺]_{ER}, suggesting that the ER of pollen tubes would contain P_{IIA}-type Ca²⁺-ATPases sensitive to CPA (Iwano et al. 2009).

Because the localization of any of P_{IIA}-type Ca²⁺ATPase in pollen is still unknown, is possible that other intracellular compartments such as Golgi apparatus, vesicles or vacuoles may also sequester Ca²⁺. For example, it was already reported in Arabidopsis seedlings that CPA inhibited the increase of [Ca²⁺] in Golgi, suggesting the presence of



in pseudo-color coding (right panels). Numbers represent time in seconds, where zero seconds corresponds to 10 min after the drug is added. Scale bar represents 10 μ m. **c** Quantitative analysis of pollen tube growth and [Ca²⁺]_{cyt} at the tip area of tomato pollen tubes after the addition of GsMTx-4. The ratio (cpVenus/ECFP) in apical (orange line) and subapical (green line) region was measured in 5- μ m² ROIs (see inset). The purple line corresponds to pollen tube elongation in the presence of GsMTx-4. Solid gray line represents the pollen tube elongation of control pollen (treated with solvent alone). "m" represents the slope from pollen growth rate. **d** Kymograph from the pollen tube presented in **b**. The vertical colored bar illustrates the ratio cpVenus/ECFP

Ca^{2+} -ATPases in Golgi (Ordenes et al. 2012). Moreover, one P_{IIA} -type Ca^{2+} ATPase from Arabidopsis, AtECA3, was localized in the Golgi apparatus when transiently expressed in tobacco epidermal leaf cells (Mills et al. 2008).

A complementary analysis was carried out with 2-aminoethoxydiphenyl borate (2-APB) a drug that, contrary to CPA, restrains Ca^{2+} movement from the ER to the cytoplasm inhibiting IP_3 receptors of the sarcoplasmic reticulum of animal cells (Maruyama et al. 1997). In plants, 2-APB inhibited Ca^{2+} spiking and root cytoplasmic streaming during nodulation in *M. truncatula* (Engstrom et al. 2002), affected hyphal growth and dissipated the tip-high cytosolic $[\text{Ca}^{2+}]$ gradient in *Neurospora crassa* (Silverman-Gavrila and Lew 2002), lowered Arabidopsis root hair cytosolic Ca^{2+} (Zhang et al. 2011) and inhibited growth of the maize pathogen *Colletotrichum graminicola* (Lange and Peiter 2016). We found that 2-APB inhibited pollen germination and pollen tube growth in a dose-dependent manner. It also induced a clear reduction in $[\text{Ca}^{2+}]_{\text{cyt}}$ at the pollen tube tip, suggesting that 2-APB has an inhibitory effect in tomato pollen tubes. Despite the fact that the presence of IP_3 receptors in plants has not been directly addressed, it was reported that IP_3 rises $[\text{Ca}^{2+}]_{\text{cyt}}$ on ER membrane preparations (Stael et al. 2012) and in pollen tubes (Franklin-Tong et al. 1996; Malhó 1998; Monteiro et al. 2005).

The influx of extracellular Ca^{2+} into the pollen tube is mediated by specific channels localized in the plasma membrane of the tip moving extracellular Ca^{2+} into the pollen tube cytoplasm increasing $[\text{Ca}^{2+}]_{\text{cyt}}$ (Wang et al. 2004; Dutta and Robinson 2004; Shang et al. 2005; Qu et al. 2007; Frietsch et al. 2007; Song et al. 2009; Michard et al. 2011; Wu et al. 2011; Hamilton et al. 2015; Gao et al. 2016). Stretch-activated Ca^{2+} channels open in response to the deformation of the plasma membrane caused during tip growth (Cardenas et al. 2008; Hamilton et al. 2015). It has been shown in pollen grains protoplasts and pollen tubes spheroplasts of *L. longiflorum* that when these channels were inhibited by a crude spider venom, pollen tube growth and influx of extracellular Ca^{2+} into the tip were blocked (Dutta and Robinson 2004). In tomato, we found that pure GsMTx-4, an active compound of the spider's venom, inhibited pollen germination in a dose-dependent manner, while the effect on pollen tube length was heterogeneous. This heterogeneous behavior was previously described when pollen tubes of *Petunia hybrida* were incubated with varying concentrations of verapamil, an inhibitor of voltage-dependent channels, other type of pollen tube plasma membrane calcium channels (Geitmann and Cresti 1998). Inhibited pollen tubes with GsMTx-4 showed reduced $[\text{Ca}^{2+}]_{\text{cyt}}$ at the tip. These results suggest that tomato stretch-activated Ca^{2+} channels are involved in the influx of calcium to the pollen tube cytoplasm maintaining the calcium gradient.

Taking all our results together, we showed that tomato pollen tube has an oscillatory growth, and that growth is inhibited when tip-focused $[\text{Ca}^{2+}]_{\text{cyt}}$ gradient is disrupted directly or indirectly with pharmacological drugs. Future research will be needed to reveal the regulation of the complicated Ca^{2+} signaling network in pollen tubes.

Author contribution statement MB and JM conceived the experiments. MB, LS, JE, MO, LP, WT and JM designed the research. WJ and WT generated the Cameleon transgenic line. MB and LS performed the experiments. MB, LS, WJ, SM, EM, SD, JE, MO, LP, WT and JM analyzed and interpreted the data. MB and JM wrote the manuscript.

Acknowledgements We thank Prof. Yongfei Wang at Shanghai Institute of Plant Physiology for providing YC 3.6 plasmid.

Funding JM was supported by Grants PICT 2012-0007, PICT2014-0423 and PICT2015-0078. WT was supported by NSFC 3157-318.


References

- Barberini ML, Muschietti J (2015) Imaging of calcium dynamics in pollen tube cytoplasm. *Methods Mol Biol* 1242:49–57. https://doi.org/10.1007/978-1-4939-1902-4_4
- Bonza MC, Loro G, Behera S, Wong A, Kudla J, Costa A (2013) Analyses of Ca^{2+} accumulation and dynamics in the endoplasmic reticulum of Arabidopsis root cells using a genetically encoded Cameleon sensor. *Plant Physiol* 163:1230–1241. <https://doi.org/10.1104/pp.113.226050>
- Capoen W, Den Herder J, Sun J, Verplancke C, De Keyser A et al (2009) Calcium spiking patterns and the role of the calcium/calmodulin-dependent kinase CCaMK in lateral root base nodulation of *Sesbania rostrata*. *Plant Cell* 21(5):1526–1540. <https://doi.org/10.1105/tpc.109.066233>
- Cardenas L, Lovy-Wheeler A, Kunkel JG, Hepler PK (2008) Pollen tube growth oscillations and intracellular calcium levels are reversibly modulated by actin polymerization. *Plant Physiol* 146:1611–1621. <https://doi.org/10.1104/pp.107.113035>
- Damineli DSC, Portes MT, Feijó JA (2017) Oscillatory signatures underlie growth regimes in Arabidopsis pollen tubes: computational methods to estimate tip location, periodicity, and synchronization in growing cells. *J Exp Bot* 68(12):3267–3281. <https://doi.org/10.1093/jxb/erx032>
- Dutta R, Robinson KR (2004) Identification and characterization of stretch-activated ion channels in pollen protoplasts. *Plant Physiol* 135:1398–1406. <https://doi.org/10.1104/pp.104.041483>
- Engstrom EM, Ehrhardt DW, Mitra RM, Long SR (2002) Pharmacological analysis of nod factor-induced calcium spiking in *Medicago truncatula*. Evidence for the requirement of type IIA calcium pumps and phosphoinositide signaling. *Plant Physiol* 128:1390–1401. <https://doi.org/10.1104/pp.010691>
- Franklin-Tong VE, Drobak BK, Allan AC, Watkins P, Trewavas AJ (1996) Growth of pollen tubes of *Papaver rhoeas* is regulated by a slow-moving calcium wave propagated by inositol 1,4,5-trisphosphate. *Plant Cell* 8:1305–1321. <https://doi.org/10.1105/tpc.8.8.1305>

- Frietsch S, Wang YF, Sladek C, Poulsen LR, Romanowsky SM, Schroeder JI et al (2007) A cyclic nucleotide-gated channel is essential for polarized tip growth of pollen. *Proc Natl Acad Sci USA* 104:14531–14536. <https://doi.org/10.1073/pnas.0701781104>
- Gao QF, Gu LL, Wang HQ, Fei CF, Fang X, Hussain J et al (2016) Cyclic nucleotide-gated channel 18 is an essential Ca^{2+} channel in pollen tube tips for pollen tube guidance to ovules in *Arabidopsis*. *Proc Natl Acad Sci USA* 113(11):3096–3101. <https://doi.org/10.1073/pnas.1524629113>
- Geisler M, Axelsen KB, Harper JF, Palmgren MG (2000) Molecular aspects of higher plant P-type Ca^{2+} -ATPases. *Biochim Biophys Acta* 1465:52–78
- Geitmann A, Cresti M (1998) Ca^{2+} channels control the rapid expansions in pulsating growth of *Petunia hybrida* pollen tubes. *J Plant Physiol* 152:439–447
- Hamilton ES, Jensen GS, Maksaev G, Katims A, Sherp AM, Haswell ES (2015) Mechanosensitive channel MSL8 regulates osmotic forces during pollen hydration and germination. *Science* 350:438–441. <https://doi.org/10.1126/science.aac6014>
- Hepler PK, Winship LJ (2015) The pollen tube clear zone: clues to the mechanism of polarized growth. *J Integr Plant Biol* 57:79–92. <https://doi.org/10.1111/jipb.12315>
- Hepler PK, Kunkel JG, Rounds CM, Winship LJ (2012) Calcium entry into pollen tubes. *Trends Plant Sci* 17:32–38. <https://doi.org/10.1016/j.tplants.2011.10.007>
- Hoekema A, Roelvink PW, Hooykaas PJJ, Schilperoort RA (1984) Delivery of T-DNA from the *Agrobacterium tumefaciens* chromosome into plant cells. *EMBO J* 3:2485–2490
- Holdaway-Clarke TL, Feijó JA, Hackett GR, Kunkel JG, Hepler PK (1997) Pollen tube growth and the intracellular cytosolic calcium gradient oscillate in phase while extracellular calcium influx is delayed. *Plant Cell* 9:1999–2010. <https://doi.org/10.1105/tpc.9.11.1999>
- Holdaway-Clarke TL, Weddle NM, Kim S, Robi A, Parris C, Kunkel JG et al (2003) Effect of extracellular calcium, pH and borate on growth oscillations in *Lilium formosanum* pollen tubes. *J Exp Bot* 54:65–72
- Iwano M, Shiba H, Miwa T, Che FS, Takayama S, Nagai T et al (2004) Ca^{2+} dynamics in a pollen grain and papilla cell during pollination of *Arabidopsis*. *Plant Physiol* 136:3562–3571. <https://doi.org/10.1104/pp.104.046961>
- Iwano M, Entani T, Shiba H, Kakita M, Nagai T, Mizuno H et al (2009) Fine-tuning of the cytoplasmic Ca^{2+} concentration is essential for pollen tube growth. *Plant Physiol* 150:1322–1334. <https://doi.org/10.1104/pp.109.139329>
- Lange M, Peiter E (2016) Cytosolic free calcium dynamics as related to hyphal and colony growth in the filamentous fungal pathogen *Colletotrichum graminicola*. *Fungal Genet Biol* 91:55–65. <https://doi.org/10.1016/j.fgb.2016.04.001>
- Liang F, Sze H (1998) A high-affinity Ca^{2+} pump, ECA1, from the endoplasmic reticulum is inhibited by cyclopiazonic acid but not by thapsigargin. *Plant Physiol* 118:817–825. <https://doi.org/10.1104/pp.118.3.817>
- Malhó R (1998) Role of 1,4,5-inositol triphosphate-induced Ca^{2+} release in pollen tube orientation. *Sex Plant Reprod* 11:231–235. <https://doi.org/10.1007/s004970050145>
- Malhó R, Trewavas AJ (1996) Localized apical increases of cytosolic free calcium control pollen tube orientation. *Plant Cell* 8:1935–1949. <https://doi.org/10.1105/tpc.8.11.1935>
- Martinez-Azorin F (2004) Cyclopiazonic acid reduces the coupling factor of the Ca^{2+} -ATPase acting on Ca^{2+} binding. *FEBS Lett* 576:73–76. <https://doi.org/10.1016/j.febslet.2004.08.064>
- Maruyama T, Kanaji T, Nakade S, Kanno T, Mikoshiba K (1997) 2-APB, 2-aminoethoxydiphenyl borate, a membrane-penetrable modulator of $\text{Ins}(1,4,5)\text{P}_3$ -induced Ca^{2+} release. *J Biochem* 122:498–505
- McCormick S (1992) Transformation of tomato with *Agrobacterium tumefaciens*. In: Lindsey K (ed) *Plant Tissue Culture Manual*. Supplement 1. Section B Number 6. Kluwer Academic Publishers, pp 1–9
- Messerli M, Robinson KR (1997) Tip localized Ca^{2+} pulses are coincident with peak pulsatile growth rates in pollen tubes of *Lilium longiflorum*. *J Cell Sci* 110:1269–1278
- Messerli MA, Creton R, Jaffe LF, Robinson KR (2000) Periodic increases in elongation rate precede increases in cytosolic Ca^{2+} during pollen tube growth. *Dev Biol* 222:84–98. <https://doi.org/10.1006/dbio.2000.9709>
- Michard E, Dias P, Feijó JA (2008) Tobacco pollen tubes as cellular models for ion dynamics: improved spatial and temporal resolution of extracellular flux and free cytosolic concentration of calcium and protons using pFluorin and YC3.1 CaMeleon. *Sex Plant Reprod* 21:169–181. <https://doi.org/10.1007/s00497-008-0076-x>
- Michard E, Lima PT, Borges F, Silva AC, Portes MT, Carvalho JE et al (2011) Glutamate receptor-like genes form Ca^{2+} channels in pollen tubes and are regulated by pistil D-serine. *Science* 332:434–437. <https://doi.org/10.1126/science.1201101>
- Mills RF, Doherty ML, Lopez-Marques RL, Weimar T, Dupree P, Palmgren MG et al (2008) ECA3, a golgi-localized P_{2A} -type ATPase, plays a crucial role in manganese nutrition in *Arabidopsis*. *Plant Physiol* 146:116–128. <https://doi.org/10.1104/pp.107.110817>
- Monteiro D, Liu Q, Lisboa S, Scherer GEF, Quader H, Malho R (2005) Phosphoinositides and phosphatidic acid regulate pollen tube growth and reorientation through modulation of $[\text{Ca}^{2+}]_c$ and membrane secretion. *J Exp Bot* 56:1665–1674. <https://doi.org/10.1093/jxb/eri163>
- Muschietti J, Eyal Y, McCormick S (1998) Pollen tube localization implies a role in pollen-pistil interactions for the tomato receptor-like protein kinases LePRK1 and LePRK2. *Plant Cell* 10:319–330. <https://doi.org/10.1105/tpc.10.3.319>
- Nagai T, Yamada S, Tominaga T, Ichikawa M, Miyawaki A (2004) Expanded dynamic range of fluorescent indicators for Ca^{2+} by circularly permuted yellow fluorescent proteins. *Proc Natl Acad Sci USA* 101:10554–10559. <https://doi.org/10.1073/pnas.0400417101>
- Ordenes VR, Moreno I, Maturana D, Norambuena L, Trewavas A, Orellana A (2012) In vivo analysis of the calcium signature in the plant Golgi apparatus reveals unique dynamics. *Cell Calcium* 52:397–404. <https://doi.org/10.1016/j.ceca.2012.06.008>
- Pierson ES, Miller DD, Callahan DA, van Aken J, Hackett G, Hepler PK (1996) Tip localized calcium entry fluctuates during pollen tube growth. *Dev Biol* 174:160–173. <https://doi.org/10.1006/dbio.1996.0060>
- Plenge-Tellechea F, Soler F, Fernandez-Belda F (1997) On the inhibition mechanism of sarcoplasmic or endoplasmic reticulum Ca^{2+} -ATPases by cyclopiazonic acid. *J Biol Chem* 272:2794–2800. <https://doi.org/10.1074/jbc.272.5.2794>
- Qu HY, Zhang ZL, Zhang SL, Liu LM, Wu JY (2007) Identification of hyperpolarization-activated calcium channels in apical pollen tubes of *Pyrus pyrifolia*. *New Phytol* 174:524–536. <https://doi.org/10.1111/j.1469-8137.2007.02069.x>
- Schiott M, Romanowsky SM, Baekgaard L, Jakobsen MK, Palmgren MG, Harper JF (2004) A plant plasma membrane Ca^{2+} pump is required for normal pollen tube growth and fertilization. *Proc Natl Acad Sci USA* 101:9502–9507. <https://doi.org/10.1073/pnas.0401542101>
- Seidler NW, Jona I, Vegh M, Martonosi A (1989) Cyclopiazonic acid is a specific inhibitor of the Ca^{2+} -ATPase of sarcoplasmic reticulum. *J Biol Chem* 264:17816–17823
- Shang ZL, Ma LG, Zhang HL, He RR, Wang XC, Cui SJ et al (2005) Ca^{2+} influx into lily pollen grains through a hyperpolarization-activated Ca^{2+} -permeable channel which can be regulated by

- extracellular CaM. *Plant Cell Physiol* 46:598–608. <https://doi.org/10.1093/pcp/pci063>
- Silverman-Gavrila LB, Lew RR (2002) An IP₃-activated Ca²⁺ channel regulates fungal tip growth. *J Cell Sci* 115:5013–5025
- Song LF, Zou JJ, Zhang WZ, Wu WH, Wang Y (2009) Ion transporters involved in pollen germination and pollen tube tip-growth. *Plant Signal Behav* 4:1193–1195
- Stael S, Wurzinger B, Mair A, Mehler N, Vothknecht UC, Teige M (2012) Plant organellar calcium signalling: an emerging field. *J Exp Bot* 63:1525–1542. <https://doi.org/10.1093/jxb/err394>
- Suchyna TM, Johnson JH, Hamer K, Leykam JF, Gage DA, Clemo HF, Baumgarten CM, Sachs F (2000) Identification of a peptide toxin from *Grammostola spatulata* spider venom that blocks cation-selective stretch-activated channels. *J Gen Physiol* 115:583–598. <https://doi.org/10.1085/jgp.115.5.583>
- Sze H, Liang F, Hwang I, Curran AC, Harper JF (2000) Diversity and regulation of plant Ca²⁺ pumps: insights from expression in yeast. *Annu Rev Plant Physiol Plant Mol Biol* 51:433–462. <https://doi.org/10.1146/annurev.arplant.51.1.433>
- Twell D, Yamaguchi J, McCormick S (1990) Pollen-specific gene expression in transgenic plants: coordinate regulation of two different tomato gene promoters during microsporogenesis. *Development* 109:705–713
- Wang YF, Fan LM, Zhang WZ, Zhang W, Wu WH (2004) Ca²⁺-permeable channels in the plasma membrane of Arabidopsis pollen are regulated by actin microfilaments. *Plant Physiol* 136:3892–3904. <https://doi.org/10.1104/pp.104.042754>
- Wu J, Qu H, Jin C, Shang Z, Wu J, Xu G, Gao Y, Zhang S (2011) cAMP activates hyperpolarization-activated Ca²⁺ channels in the pollen of *Pyrus pyrifolia*. *Plant Cell Rep* 30(7):1193–1200. <https://doi.org/10.1007/s00299-011-1027-9>
- Zhang J, Vanneste S, Brewer PB, Michniewicz M, Grones P et al (2011) Inositol trisphosphate-induced Ca²⁺ signaling modulates auxin transport and PIN polarity. *Dev Cell* 20:855–866. <https://doi.org/10.1016/j.devcel.2011.05.013>

Affiliations

María Laura Barberini¹ · Lorena Sigaut² · Weijie Huang^{3,7} · Silvina Mangano⁴ · Silvina Paola Denita Juarez⁴ · Eliana Marzol⁴ · José Estevez⁴ · Mariana Obertello¹ · Lía Pietrasanta^{2,5} · Weihua Tang³ · Jorge Muschietti^{1,6} 

¹ Instituto de Investigaciones en Ingeniería Genética y Biología Molecular, “Dr. Héctor Torres” (INGEBI-CONICET), Vuelta de Obligado 2490, C1428ADN Buenos Aires, Argentina

² Instituto de Física de Buenos Aires (IFIBA-CONICET), Departamento de Física, Facultad de Ciencias Exactas y Naturales, Universidad de Buenos Aires, Intendente Güiraldes 2160, Ciudad Universitaria, Pabellón I, C1428EHA Buenos Aires, Argentina

³ National Key Laboratory of Plant Molecular Genetics, Center for Excellence in Molecular Plant Sciences, Institute of Plant Physiology and Ecology, Shanghai Institutes for Biological Sciences, Chinese Academy of Sciences, 300 Fenglin Road, Shanghai 200032, China

⁴ Fundación Instituto Leloir and Instituto de Investigaciones Bioquímicas de Buenos Aires (IIBBA-CONICET), Av. Patricias Argentinas 435, CP C1405BWE Buenos Aires, Argentina

⁵ Centro de Microscopías Avanzadas, Facultad de Ciencias Exactas y Naturales, Universidad de Buenos Aires, Intendente Güiraldes 2160, Ciudad Universitaria, Pabellón I, C1428EHA Buenos Aires, Argentina

⁶ Departamento de Biodiversidad y Biología Experimental, Facultad de Ciencias Exactas y Naturales, Universidad de Buenos Aires, Intendente Güiraldes 2160, Ciudad Universitaria, Pabellón II, C1428EGA Buenos Aires, Argentina

⁷ Present Address: Department of Cell and Developmental Biology, John Innes Centre, Norwich Research Park, Norwich NR4 7UH, United Kingdom